

PION PRODUCTION BY NEGATIVE PIONS\*

Barry C. Barish, Richard J. Kurz, Paul G. McManigal, Victor Perez-Mendez,<sup>†</sup> and Julius Solomon  
Lawrence Radiation Laboratory, University of California, Berkeley, California

(Received February 13, 1961)

The reaction  $\pi^- + p \rightarrow \pi^- + \pi^+ + n$ , for  $T_\pi$  incident = 365 Mev and 432 Mev, was studied. In a previous experiment Perkins *et al.* investigated this reaction.<sup>1</sup> Their total cross section was much larger than predicted by static-model theory. Rodberg suggested that the large difference between experiment and theory was explainable by the inclusion of a pion-pion interaction.<sup>2</sup> Perkins also noted a possible deviation of the energy spectrum of the observed pion from a statistical distribution. The significant interactions at these energies are

$$\pi^- + p \rightarrow \pi^- + p, \quad (1a)$$

$$\rightarrow \pi^0 + n, \quad (1b)$$

$$\rightarrow \pi^- + \pi^+ + n, \quad (1c)$$

$$\rightarrow \pi^- + \pi^0 + p, \quad (1d)$$

$$\rightarrow \pi^0 + \pi^0 + n. \quad (1e)$$

The  $\pi^+$  from Reaction (1c) with  $30 \text{ Mev} \leq T_{\pi^+} \leq 180 \text{ Mev}$  was observed at  $\theta = 20, 50, 80,$  and  $110$  degrees. The energy of the  $\pi^+$  was determined by a magnetic spectrometer.

The  $\pi^-$  incident beam was produced by the primary proton beam of the Berkeley 184-inch synchrocyclotron striking an internal Be target. A doublet quadrupole magnet located inside the shielding of the accelerator was used astigmatically to compensate the effects of the main field

of the machine and yield a parallel beam outside the shielding. The  $\pi^-$  beam was momentum-analyzed by a 40-deg bend in an  $H$  magnet and focused at the target by a doublet quadrupole magnet. After collimation the cross section of the beam was  $\frac{3}{4} \text{ in.} \times 1\frac{3}{4} \text{ in.}$  The properties of the pion beams as determined by range curves and calculations are listed in Table I. The liquid hydrogen target was a 4-in long 2-in. diameter Mylar cylinder whose axis lay along the beam direction. The target was constructed so that 300 deg could be viewed in the laboratory, obstructed by only 0.031 in. of Mylar. The experimental arrangement of the target area is shown in Fig. 1. For the spectrometer, a  $C$  magnet with  $13 \times 24$ -in. pole pieces and a 4-in. gap (maximum field = 19 kgauss) was used in a wedge configuration<sup>3</sup> to obtain focusing in the horizontal plane. The  $\pi_i, \pi_i'$  counters were located at the image of the target for a momentum corresponding to the desired  $\pi^+$  energy. The energy resolution and solid angle

Table I. Properties of  $\pi^-$  beams.

Energy (Mev)	Percent $\mu^-$	Percent $e^-$	Intensity
$365 \pm 15$	4.1	1.0	$3 \times 10^6/\text{min}$
$432 \pm 15$	3.8	1.0	$1 \times 10^6/\text{min}$

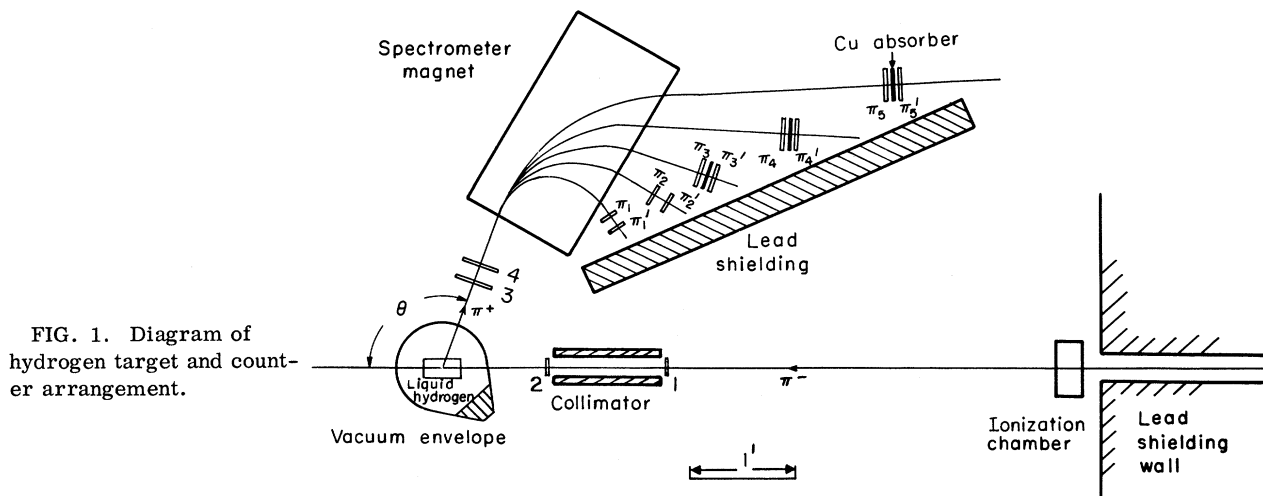


FIG. 1. Diagram of hydrogen target and counter arrangement.

of the  $\pi^+$  channels were determined to within  $\pm 5\%$  by wire-orbit measurements. A  $\pi^+$  count required a coincidence ( $1234\pi_i\pi_i'$ ). Protons with momentum equal to the  $\pi^+$  momentum were excluded by appropriate thicknesses of Cu absorber inserted between  $\pi_i$  and  $\pi_i'$ . For the monitor coincidences (12) a fast coincidence (4-nsec resolving time) followed by a 40-Mc/sec transistorized discriminator-scaler circuit was used. The high  $\pi^-$  beam intensities and cyclotron beam rf fine structure introduced problems in direct counter monitoring of the  $\pi^-$  beam. Therefore, a thin-walled ionization chamber was used as an absolute monitor, and was calibrated versus the (12) coincidences at lower beam intensities. The accuracy of the monitor was  $\pm 2\%$  at 365 Mev and  $\pm 0.5\%$  at 432 Mev.

The  $\pi^+$ -detection system did not exclude positrons of the proper momentum resulting from Reaction (1b) either by conversion of  $\gamma$  rays from the usual decay ( $\pi^0 \rightarrow \gamma + \gamma$ ) or directly through Dalitz decay ( $\pi^0 \rightarrow \gamma + e^+ + e^-$ ). The number of conversion  $e^+$  was experimentally determined by inserting Cu converting material between the target and Counter 3 in multiples of the amount of converting material in the target ( $\approx 0.01$  radiation length). The slope of the plot of yield vs converting material indicates the number of conversion  $e^+$  entering the spectrometer magnet. These measurements were made at  $\theta = 20$  deg for 365 Mev and 432 Mev. The measured values agreed with calculations of  $d^2\sigma/dE d\Omega$  for conversion  $e^+$  made using the differential cross-section data on  $\pi^- + p \rightarrow \pi^0 + n$  by Caris et al.<sup>4</sup>  $d^2\sigma/dE d\Omega$  for Dalitz  $e^+$  was also calculated by using the Caris data and the energy and angular distribution of the Dalitz  $e^+$  in the  $\pi^0$  rest system.<sup>5</sup> The total positron contamination at  $\theta = 20$  deg was  $\approx 0.17$  at 365 Mev and  $\approx 0.12$  at 432 Mev. The values decrease rapidly as  $\theta$  increases. The calculated values were used to correct the data. The efficiency of the  $\pi^+$  detection system was calculated. Losses of  $\pi^+ \rightarrow \mu^+ + \nu$  ( $\approx 2\%$  to  $7\%$ ), Coulomb scattering, and nuclear absorption of the  $\pi^+$  were taken into account.

The results for  $d^2\sigma/dT^* d\Omega^*$ ,  $d\sigma/d\Omega^*$ , and  $\sigma_{\text{total}}$  are presented in Table II. Figure 2 illustrates a typical  $\pi^+$  energy distribution along with a phase-space statistical distribution normalized to give equal  $d\sigma/d\Omega^*$ . At 365 Mev,  $d\sigma/d\Omega^*$  is isotropic. At 432 Mev,  $d\sigma/d\Omega^*$  was fitted to a curve of the form  $a_0 + a_1 \cos\theta^*$ . The coefficients  $a_0$ ,  $a_1$  obtained by the least-squares method are presented

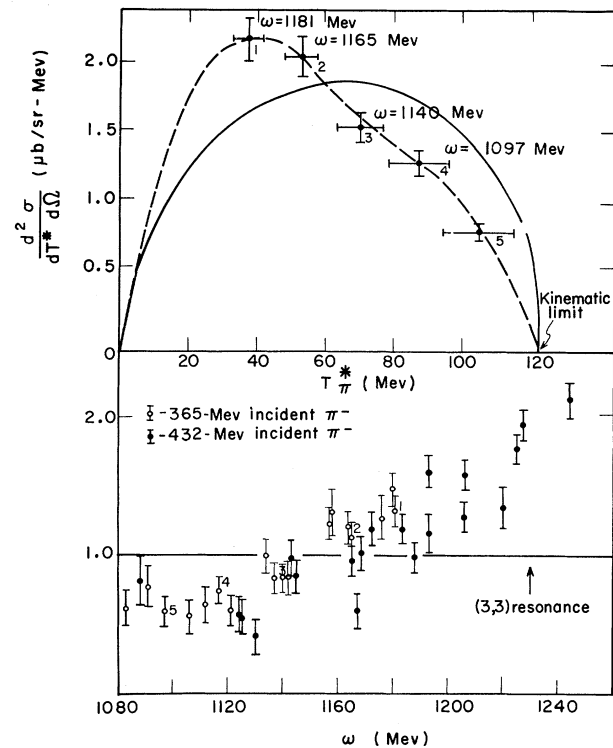


FIG. 2. (a)  $d^2\sigma/dT^* d\Omega^*$  versus  $T^*$  for  $T_{\pi^-}$  incident = 365 Mev and  $\theta_{\pi^+} = 50$  deg. The solid curve is a phase-space distribution normalized to  $d\sigma/d\Omega^*$ . (b) The ratio of  $d^2\sigma/dT^* d\Omega^*$  (observed) and normalized  $d^2\sigma/dT^* d\Omega^*$  (phase space) versus  $\omega$ , the total energy for the  $\pi^-$  and neutron in their barycentric system. The errors indicated include that of  $d^2\sigma/dT^* d\Omega^*$  and the uncertainty in the normalization of  $d^2\sigma/dT^* d\Omega^*$  phase space.

in Table III with those of Perkins et al.<sup>1</sup> for comparison.

The total cross sections agree with Perkins et al.<sup>1</sup> and therefore substantiate the experimental deviation from calculations based on static models.<sup>6</sup> The inclusion of a pion-pion interaction by Rodberg<sup>2</sup> produces agreement with the measured total cross sections but predicts a pion energy spectrum favoring higher energies than phase-space statistical distributions. The striking feature of the measured  $\pi^+$  energy distributions is the low-energy peaking. The laboratory-system energy and angle of the observed  $\pi^+$  determines  $\omega$ , the total energy of the  $\pi^-$ , and  $n(T = 3/2)$  in their barycentric system.<sup>7</sup> The isobar model<sup>8</sup> assumes that final-state  $\pi$ - $N$  combinations in the resonant state ( $T = 3/2$ ,  $J = 3/2$ ,  $\omega = 1230$  Mev) are preferred.

Table II. Differential cross sections with respect to  $\pi^+$  energy and angle;  $\pi^+$  angle; and total cross sections (the asterisk denotes total center-of-mass quantity).

$T_{\pi \text{ inc.}}$ (Mev)	$\theta$ (deg)	$T^*$ (Mev)	$\theta^*$ (deg)	$d^2\sigma/dT^*d\Omega^*$ ( $\mu\text{b}/\text{sr-Mev}$ )	$d\sigma/d\Omega^*$ ( $\mu\text{b}/\text{sr}$ )	$\sigma_T$ (mb)	
365 $\pm$ 15	20	35 $\pm$ 4.2	33	2.26 $\pm$ 0.19	168 $\pm$ 14	2.07 $\pm$ 0.09	
		48 $\pm$ 6.0	31.5	2.04 $\pm$ 0.17			
		65.5 $\pm$ 6.8	31	1.48 $\pm$ 0.13			
		83.5 $\pm$ 8.2	30.5	1.00 $\pm$ 0.08			
	50	37.5 $\pm$ 4.3	78.5	2.17 $\pm$ 0.16	174 $\pm$ 13		
		52.5 $\pm$ 4.8	75.3	2.05 $\pm$ 0.15			
		70.2 $\pm$ 7.0	73	1.53 $\pm$ 0.11			
		87.3 $\pm$ 8.6	71.5	1.27 $\pm$ 0.09			
		105 $\pm$ 11.5	70.5	0.77 $\pm$ 0.06			
	80	37.5 $\pm$ 1.2	116	1.87 $\pm$ 0.23	148 $\pm$ 14		
		53.7 $\pm$ 3.2	109	1.99 $\pm$ 0.15			
		71.0 $\pm$ 5.3	107.5	1.29 $\pm$ 0.09			
		96.2 $\pm$ 6.1	105	0.69 $\pm$ 0.06			
		115.0 $\pm$ 5.1	104	0.45 $\pm$ 0.05			
	110	53.0 $\pm$ 2.5	138	2.29 $\pm$ 0.31	168 $\pm$ 17		
		76.1 $\pm$ 4.3	135	1.82 $\pm$ 0.13			
		96.0 $\pm$ 7.2	133	0.98 $\pm$ 0.08			
		115.0 $\pm$ 4.5	132	0.73 $\pm$ 0.08			
	432 $\pm$ 15	20	19.5 $\pm$ 3.3	37	3.11 $\pm$ 0.33	297 $\pm$ 24	3.26 $\pm$ 0.14
			35.0 $\pm$ 4.3	34.5	3.81 $\pm$ 0.32		
53.0 $\pm$ 6.1			33	3.67 $\pm$ 0.27			
69.5 $\pm$ 8.5			32	2.46 $\pm$ 0.20			
90.0 $\pm$ 8.5			31	1.51 $\pm$ 0.14			
50		35.0 $\pm$ 4.0	83	3.21 $\pm$ 0.24	277 $\pm$ 22		
		51.5 $\pm$ 5.0	78	2.74 $\pm$ 0.21			
		68.7 $\pm$ 8.5	74.5	2.88 $\pm$ 0.20			
		86.5 $\pm$ 8.3	73	2.21 $\pm$ 0.16			
		115.3 $\pm$ 9.7	72	0.81 $\pm$ 0.08			
80		38.5 $\pm$ 2.3	116	2.20 $\pm$ 0.27	239 $\pm$ 22		
		61.0 $\pm$ 3.6	110	3.16 $\pm$ 0.25			
		79.3 $\pm$ 5.5	108	2.47 $\pm$ 0.18			
		101.0 $\pm$ 7.5	106	1.76 $\pm$ 0.13			
		117.3 $\pm$ 8.8	105	0.95 $\pm$ 0.09			
110		58.2 $\pm$ 3.2	132.5	2.17 $\pm$ 0.21	232 $\pm$ 23		
		81.0 $\pm$ 4.3	131.5	2.04 $\pm$ 0.16			
		101.5 $\pm$ 5.5	130.6	1.88 $\pm$ 0.14			
		126.8 $\pm$ 9.0	130.5	0.85 $\pm$ 0.07			
		146.7 $\pm$ 5.0	130.5	0.56 $\pm$ 0.09			

At our incident  $\pi^-$  energies the total center-of-mass energy available requires a low-energy  $\pi^+$  if  $\omega$  is to approach 1230 Mev. The low-energy peaking agrees with the qualitative predictions of the isobar models. In Fig. 2(b), the ratio of  $d^2\sigma/dT^*d\Omega^*$  (observed) to  $d^2\sigma/dT^*d\Omega^*$  (phase space) is plotted versus  $\omega$  for all experimental points at both energies. The increase of this ratio in the region of the (3, 3) pion-nucleon

resonance is pronounced. Anisovich<sup>9</sup> has presented a model which explains the enhanced total cross section for Reaction (1c) and the strong influence of the (3, 3) resonance on the  $\pi^+$  differential distributions, using only the resonant pion-nucleon final-state interaction.

We should like to acknowledge the continued interest and support of Professor A. C. Helmholz and Professor Burton J. Moyer. We also wish to

Table III. Least-squares-fit coefficients for  $d\sigma/d\Omega^* = a_0 + a_1 \cos\theta^*$  at  $T_{\pi^-}$  incident = 432 Mev.

	$a_0$ ( $\mu\text{b}/\text{sr}$ )	$a_1$ ( $\mu\text{b}/\text{sr}$ )
This experiment	$259 \pm 11$	$47 \pm 21$
Perkins <i>et al.</i>	$268 \pm 20$	$138 \pm 36$

thank Mr. James Vale and the cyclotron crew for their assistance and cooperation during the course of the experiment.

\*Work done under the auspices of the U. S. Atomic Energy Commission.

†Present address: Hebrew University, Jerusalem, Israel.

<sup>1</sup>W. A. Perkins, J. C. Caris, R. W. Kenney, E. Knapp, and V. Perez-Mendez, Phys. Rev. Letters

**3**, 56 (1959); W. A. Perkins, J. C. Caris, R. W. Kenney, and V. Perez-Mendez, Phys. Rev. **118**, 1364 (1960).

<sup>2</sup>L. S. Rodberg, Phys. Rev. Letters **3**, 58 (1959).

<sup>3</sup>W. G. Cross, Rev. Sci. Instr. **22**, 717 (1951).

<sup>4</sup>J. C. Caris, R. W. Kenney, V. Perez-Mendez, and W. A. Perkins, Phys. Rev. **121**, 893 (1961).

<sup>5</sup>R. H. Dalitz, Proc. Roy. Soc. (London) **A64**, 667 (1951).

<sup>6</sup>S. Barshay, Phys. Rev. **103**, 1102 (1956); J. Franklin, Phys. Rev. **105**, 1101 (1957); L. S. Rodberg, Phys. Rev. **106**, 1090 (1957); E. Kazes, Phys. Rev. **107**, 1131 (1957).

<sup>7</sup>G. F. Chew and F. E. Low, Phys. Rev. **113**, 1640 (1959).

<sup>8</sup>S. J. Lindenbaum and R. M. Sternheimer, Phys. Rev. **109**, 1723 (1958); S. Bergia, F. Bonsignori, and A. Stanghellini, Nuovo cimento **16**, 1073 (1960).

<sup>9</sup>V. V. Anisovich, J. Exptl. Theoret. Phys. U.S.S.R. **39**, 97 (1960) [translation: Soviet Phys. - JETP **12**, 71 (1961)].

### RESONANCE IN THE $K-\pi$ SYSTEM\*

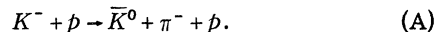
Margaret Alston, Luis W. Alvarez, Philippe Eberhard,<sup>†</sup> Myron L. Good,<sup>‡</sup>

William Graziano, Harold K. Ticho,<sup>||</sup> and Stanley G. Wojcicki

Lawrence Radiation Laboratory and Department of Physics, University of California, Berkeley, California

(Received February 16, 1961)

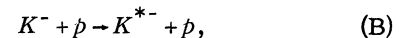
In a continuation of the study of the interaction of 1.15-Bev/c  $K^-$  mesons in hydrogen by means of the Lawrence Radiation Laboratory 15-inch hydrogen bubble chamber, we now report a study of the reaction<sup>1</sup>



Examples of this reaction were easily identified in those cases in which the  $\bar{K}^0$  decayed into charged pions and appeared in the chamber as a two-prong interaction associated with a  $V$ . A kinematic analysis isolated 48 events of reaction (A) from other events with similar topology.<sup>2</sup> In only one case was the identification not unique. Correcting for neutral decays of the  $\bar{K}^0$  and for escape from the chamber, we find a total cross section of  $2.0 \pm 0.3$  mb for Reaction (A).

The events are shown on a Dalitz plot in Fig. 1. If the reaction were entirely dominated by phase space, the Dalitz plot would be uniformly populated. Instead, a strong clumping around proton kinetic energy of 20 Mev is observed. This effect cannot be explained by an interaction matrix element that increases monotonically with decreasing proton energy. Whereas an extrapolation from the region  $15 \text{ Mev} \leq T_p \leq 25 \text{ Mev}$  would lead

one to expect a minimum of 16 events in the region  $T_p \leq 15 \text{ Mev}$ , only three are found there. No experimental bias against very low energy protons in the  $K-p$  center-of-mass system can exist, since such protons have laboratory-system momenta of approximately 600 Mev/c, and are easily identified. The observed distribution can best be explained by a quasi-two-body reaction of the type



followed by a decay,



The 3-3 resonance of the pion-nucleon system would show itself on the Dalitz plot as a concentration of points along the diagonal line drawn through Fig. 1. The absence of any evidence for this resonance in our data can be explained if Reaction (A) proceeds primarily through the  $I=0$  channel, which cannot produce a  $p-\pi^-$  system in the  $I=3/2$  state. Further, even in the  $I=1$  channel, the 3-3 resonance favors  $(n + \pi^0) + \bar{K}^0$  over  $(p + \pi^-) + \bar{K}^0$ , and hence provides additional suppression of this resonance.

The mass distribution of the  $K^{*-}$  is shown in